



OPEN ACCESS

EDITED BY

Srinivasa Reddy Bonam,
University of Texas Medical Branch at
Galveston, United States

REVIEWED BY

Fergal Joseph Duffy,
Center for Infectious Disease Research,
United States
Agam Prasad Singh,
National Institute of Immunology (NII),
India

*CORRESPONDENCE

Shusaku Mizukami

✉ mizukami@nagasaki-u.ac.jp

†These authors have equally contributed to
this work

RECEIVED 05 December 2022

ACCEPTED 25 July 2023

PUBLISHED 23 August 2023

CITATION

Nakamae S, Miyagawa S, Ogawa K,
Kamiya M, Taniguchi M, Ono A,
Kawaguchi M, Teklemichael AA, Jian J-Y,
Araki T, Katagami Y, Mukai H, Annoura T,
Yui K, Hirayama K, Kawakami S and
Mizukami S (2023) Induction of liver-
resident memory T cells and protection at
liver-stage malaria by mRNA-containing
lipid nanoparticles.
Front. Immunol. 14:1116299.
doi: 10.3389/fimmu.2023.1116299

COPYRIGHT

© 2023 Nakamae, Miyagawa, Ogawa,
Kamiya, Taniguchi, Ono, Kawaguchi,
Teklemichael, Jian, Araki, Katagami, Mukai,
Annoura, Yui, Hirayama, Kawakami and
Mizukami. This is an open-access article
distributed under the terms of the [Creative
Commons Attribution License \(CC BY\)](https://creativecommons.org/licenses/by/4.0/). The
use, distribution or reproduction in other
forums is permitted, provided the original
author(s) and the copyright owner(s) are
credited and that the original publication in
this journal is cited, in accordance with
accepted academic practice. No use,
distribution or reproduction is permitted
which does not comply with these terms.

Induction of liver-resident memory T cells and protection at liver-stage malaria by mRNA- containing lipid nanoparticles

Sayuri Nakamae^{1†}, Satoshi Miyagawa^{1,2†}, Koki Ogawa^{3†},
Mariko Kamiya³, Mayumi Taniguchi¹, Akari Ono³,
Maho Kawaguchi³, Awet Alem Teklemichael¹, Jiun-Yu Jian¹,
Tamasa Araki⁴, Yukimi Katagami¹, Hidefumi Mukai³,
Takeshi Annoura⁴, Katsuyuki Yui⁵, Kenji Hirayama⁶,
Shigeru Kawakami³ and Shusaku Mizukami^{1,6*}

¹Department of Immune Regulation, Shionogi Global Infectious Diseases Division, Institute of Tropical Medicine, Nagasaki University, Nagasaki, Nagasaki, Japan, ²Laboratory for Drug Discovery and Disease Research, SHIONOGI & CO., LTD., Osaka, Japan, ³Department of Pharmaceutical Informatics, Graduate School of Biomedical Sciences, Nagasaki University, Nagasaki, Nagasaki, Japan, ⁴Department of Parasitology, National Institute of Infectious Diseases, Shinjuku-ku, Tokyo, Japan, ⁵Shionogi Global Infectious Diseases Division, Institute of Tropical Medicine, Nagasaki University, Nagasaki, Nagasaki, Japan, ⁶School of Tropical Medicine and Global Health, Nagasaki University, Nagasaki, Nagasaki, Japan

Recent studies have suggested that CD8⁺ liver-resident memory T (T_{RM}) cells are crucial in the protection against liver-stage malaria. We used liver-directed mRNA-containing lipid nanoparticles (mRNA-LNPs) to induce liver T_{RM} cells in a murine model. Single-dose intravenous injections of ovalbumin mRNA-LNPs effectively induced antigen-specific cytotoxic T lymphocytes in a dose-dependent manner in the liver on day 7. T_{RM} cells (CD8⁺ CD44^{hi} CD62L^{lo} CD69⁺ KLRG1⁺) were induced 5 weeks after immunization. To examine the protective efficacy, mice were intramuscularly immunized with two doses of circumsporozoite protein mRNA-LNPs at 3-week intervals and challenged with sporozoites of *Plasmodium berghei* ANKA. Sterile immunity was observed in some of the mice, and the other mice showed a delay in blood-stage development when compared with the control mice. mRNA-LNPs therefore induce memory CD8⁺ T cells that can protect against sporozoites during liver-stage malaria and may provide a basis for vaccines against the disease.

KEYWORDS

liver-stage malaria, vaccine, mRNA, lipid nanoparticles, resident memory T cells, cellular immunity

1 Introduction

Malaria is a serious life-threatening infectious disease. In 2020, the World Health Organization (WHO) estimated that there were 241 million cases and 627,000 deaths caused by malaria worldwide (1). Immediately after entering the human body through a mosquito bite, *Plasmodium* sporozoites invade hepatocytes and proliferate. This is known as the liver stage of malaria and is followed by the blood stage. Malaria control strategies include various approaches, such as integrated vector control, clinical management by antimalarial drugs, and preventive vaccines (2–6). However, the rapid development and spread of resistant strains of mosquitoes to insecticides and *Plasmodium* parasites to antimalarial drugs pose a threat to malaria control outcomes (7). The generation of alternative tools, including novel vaccines, is therefore needed. In 2021, the WHO recommended RTS,S/AS01 as the first malaria vaccine for children in sub-Saharan Africa and other regions with a moderate-to-high prevalence of *P. falciparum* infections (1). However, the vaccine has only exhibited modest efficacy and short-term durability and needs to be administered in four doses to achieve a maximum efficacy of 60–70% in terms of reducing clinical complications (8–10). A next-generation vaccine with promising efficacy against infections caused by *Plasmodium* parasites is therefore urgently needed.

In liver-stage malaria, CD8⁺ T cells play an important role in protection, as shown by the radiation-attenuated sporozoite (RAS) vaccine, which has been highly effective in mouse and human malaria models (11–15). The circumsporozoite protein (CSP) has been described as a major antigen in liver-stage malaria in mouse models, and its MHC I-restricted epitope has further been described (16–18). The RTS,S vaccine has been developed for pre-erythrocytic stage interruption using CSP but has been shown to stimulate the production of specific antibodies and weak T cell-mediated immunity (19). Therefore, a malaria vaccine that can effectively induce potent cytotoxic CD8⁺ T cells that are specific to the liver stage is required (20).

Resident memory CD8⁺ T (T_{RM}) cells constitute a recently-identified lymphocyte lineage that occupies tissue without recirculating (21). T_{RM} cells are the first-line defenders against reinfection by pathogens. T_{RM} cells further express unique surface markers, such as CD69, based on their localization (21–23). Recently, liver-resident T_{RM} cells have been reported to play an

important role in the protection against sporozoite infections (22). The efficient induction of T_{RM} cells in the liver may be key for the development of next-generation malaria vaccines since T_{RM} cells contribute to the protection against sporozoite infections.

Nucleic acid-based therapies have become a new trend in alternative vaccine development (24). Messenger RNA (mRNA)-based vaccinations do not pose the risks of vaccine-derived infections and insertional mutagenesis as opposed to virus-based and DNA vaccines, respectively. mRNA delivery systems to the cytoplasm of target cells have been intensively studied to protect mRNA from RNases. Among them, lipid nanoparticles (LNPs) are the most advanced mRNA carriers intended for vaccine-based therapies (25–27). The ionizable lipids in LNPs form complexes with mRNA in lipid vesicles to yield core-shell structures (28). After LNPs are taken into cells via endocytosis, the ionizable lipids in the LNPs become positively charged in response to acidification. Membrane destabilization is then promoted, and endosomal escape is facilitated to deliver the mRNA in the LNPs to the cytosol. It has also been suggested that LNPs accumulate in the liver when administered systemically via intravenous and intramuscular injections (29, 30). Through such mechanisms, LNPs can deliver intact mRNA to the cytosol for translation in the liver.

To develop a liver-stage-specific T cell-mediated vaccine, we used a liver-directed LNP-based mRNA vaccine platform and the rodent malaria parasite *P. berghei* ANKA (PbA). The mRNA-LNP vaccine was found to induce potent T_{RM} cells in the liver, which are protective against liver-stage malarial infections.

2 Materials and methods

2.1 Animals

C57BL/6N (B6) and BALB/c mice (5–9 weeks old; CLEA, Tokyo, Japan) were used for the experiments. H-2K^b-restricted OT-I transgenic mice expressing the TCR specific for SIINFEKL were provided by Dr. H. Kosaka (Osaka University, Osaka, Japan) (31). B6.SJL-Ptprc congenic (B6.SJL) mice (CD45.1⁺) were provided by Dr. Y. Takahama (University of Tokushima, Tokushima, Japan). The B6.SJL and OT-I mice were bred, and the offspring were intercrossed to obtain CD45.1⁺ OT-I mice. The mice were housed in a standard clean room under conventional conditions at the Laboratory Animal Center for Animal Research at Nagasaki University. The animal experiments were approved by the Institutional Animal Care and Use Committee of Nagasaki University and were conducted in accordance with the guidelines for Animal Experimentation at Nagasaki University.

2.2 mRNA

OVA and firefly luciferase (FLuc) mRNA were purchased from TriLink (San Diego, CA, USA). The DNA template vector for the transcription of mRNA, pSHL, was constructed by inserting the sequences of the T7 promoter, 5' UTR, IgGκ-chain signal sequence,

Abbreviations: WHO, World Health Organization; CSP, circumsporozoite protein; RAS, radiation-attenuated sporozoite; T_{RM}, resident memory CD8⁺ T; mRNA, messenger RNA; LNPs, lipid nanoparticles; PbA, *Plasmodium berghei* ANKA; B6, C57BL/6N; FLuc, firefly luciferase; PBS, phosphate-buffered saline; EE, encapsulation efficiency; FBS, fetal bovine serum; ALT, alanine aminotransferase; ELISA, enzyme-linked immunosorbent assay; ssPalm, SS-cleavable pH-activated lipid-like material; DOPC, 1,2-dioleoyl-sn-glycero-3-phosphocholine; DMG-PEG2000, 1,2-dimyristoyl-rac-glycero-3-methylpolyoxyethylene; OVA, ovalbumin; TCR, T-cell receptor; T_{EM}, effector memory CD8⁺ T cells; T_{CM}, central memory CD8⁺ T cells; GAS, genetically-attenuated sporozoites; CAS, chemically-attenuated sporozoites; PDI, polydispersity index.

haemagglutinin tag (YPYDVPDYA), EcoRI and BamHI restriction sites, 3' UTR, 120 adenosines, and SapI restriction site into the pUC-GW-Amp vector (GENEWIZ, South Plainfield, NJ, USA). The truncated CSP sequence (PBANKA_0403200) lacking 1–23 amino acids (aa) in the signal sequence, 93–201 aa in the repeat region, and 319–340 aa in the GPI anchor region was synthesized by Eurofins Genomics (Ebersberg, Germany) and inserted into pSHI via the traditional cloning method using the EcoRI and BamHI restriction enzymes (New England Biolabs, Ipswich, MA, USA). The codon usage of the sequences coding for the IgGκ-chain signal sequence, haemagglutinin tag, and CSP was optimized for *Mus musculus*. The constructed CSP template plasmid was purified from *Escherichia coli* using the EndoFree Plasmid Maxi Kit (Qiagen, Hilden, Germany) and linearized using the SapI restriction enzyme (New England Biolabs). *In-vitro* transcription was performed using the HiScribe T7 High Yield RNA Synthesis Kit (New England Biolabs) with CleanCap Reagent AG (TriLink) to cap the 5' end of the RNA. CSP mRNA was purified using LiCl precipitation after the DNase treatment. Ψ-CSP mRNA was synthesized with N¹-methylpseudouridine-5'-triphosphate (TriLink) and purified using RNeasy Mini Kit (Qiagen).

2.3 Preparation of LNP-encapsulated mRNA

LNP-encapsulated mRNA was prepared by mixing lipids and mRNA using a microfluidic system, as previously described (32). COATSOME[®] SS-OP (NOF, Tokyo, Japan), 1,2-dioleoyl-sn-glycero-3-phosphocholine (DOPC; NOF), cholesterol (Nacalai Tesque, Kyoto, Japan), and 1,2-dimyristoyl-rac-glycero-3-methylpolyoxyethylene (DMG-PEG2000; NOF) were dissolved to 4.5 mM in ethanol. The molar ratio of each lipid was 6/1/3 (SS-OP/DOPC/cholesterol), and DMG-PEG2000 was added at a concentration of 1.5% of the total lipids. The mRNA was diluted to 7.5 μg/mL in 20 mM malic acid buffer (pH 3.0). Lipid and mRNA solutions were mixed in a NanoAssembl[®] Benchtop (Precision NanoSystems, British Columbia, Canada) using a total flow rate of 4 mL/min and a flow rate ratio of 3:1 (mRNA:lipid). The resultant solution was dialyzed against MES buffer (pH 6.5) to remove ethanol and then concentrated to obtain the necessary concentration through ultrafiltration using Amicon[®] Ultra-15 (Merck, Darmstadt, Germany). The LNPs were then suspended in phosphate-buffered saline (PBS).

2.4 Characterization of LNPs

The particle size, polydispersity index, and zeta potential of the LNPs were measured using a Zetasizer Nano ZS (Malvern Instruments, Malvern, UK) as previously described (32). The LNPs were diluted 40 times in PBS and introduced into capillary cells. The measurements were then taken at 25°C. To evaluate encapsulation efficiency, mRNA was quantified using the Quant-iT RiboGreen RNA Assay Kit (Thermo Fisher Scientific, Waltham, MA, USA). The unencapsulated mRNA concentration was

measured by quantifying the intact LNPs, while the total mRNA concentration was measured after the LNPs had been solubilized using Triton X-100. Encapsulation efficiency (EE) was calculated using the following formula:

$$EE = \frac{[(\text{total mRNA}) - (\text{unencapsulated mRNA})]}{(\text{total mRNA})}$$

2.5 *In-vivo* distribution of FLuc mRNA-LNPs

To assess the changes in the FLuc mRNA-LNPs over time, BALB/c mice were inoculated with FLuc mRNA-LNPs (5 μg) intravenously, intramuscularly, or subcutaneously. To detect luminescence, the mice were administered 150 mg/kg of D-luciferin (Syd labs, Hopkinton, MA, USA) intraperitoneally and anaesthetized with a mixture of oxygen and isoflurane (Wako, Osaka, Japan). Ten minutes after the administration of D-luciferin, the mice were imaged using IVIS Lumina II (Caliper Life Sciences, Waltham, MA, USA) with an exposure time of 5 s. To detect the tissue distribution of the FLuc mRNA-LNPs, B6 mice were intravenously inoculated with FLuc mRNA-LNPs (5 μg) and administered D-luciferin (150 mg/kg) intraperitoneally 3 h later. The reaction was observed for 10 min. The brains, hearts, livers, spleens, lungs, kidneys, and intestines were collected immediately and imaged using an IVIS imager for 5 s. Bioluminescent signals in the regions of interest were quantified using Living Image 3.0 (Caliper Life Sciences).

2.6 Adaptive transfer and immunization

OT-I CD8⁺ cells were isolated using the BD[™] IMag cell separation system as previously described (33). In brief, CD8⁺ (> 95%) cells were prepared from the spleen, brachial, and inguinal lymph nodes of the CD45.1⁺ OT-I mice using anti-CD8 IMag (BD Biosciences, Franklin, NJ, USA) and injected into the tail veins of the B6 mice (1 × 10⁶/mouse). Two days later, the mice were immunized with OVA mRNA-LNPs intravenously, intramuscularly, or subcutaneously. The BALB/c mice were intramuscularly immunized with 3.35 μg of CSP mRNA-LNPs or 6.7 μg of Ψ-CSP mRNA-LNPs at 3-week intervals.

2.7 Tissue processing for T-cell analysis

The mice were anaesthetized with a combination of 0.75 mg/kg of medetomidine hydrochloride (Kyoritsu Seiyaku, Tokyo, Japan), 4 mg/kg of midazolam (Sandoz K.K., Tokyo, Japan), and 5 mg/kg of butorphanol tartrate (Meiji Seika Pharma Co., Ltd., Tokyo, Japan), in addition to the inhalation of isoflurane (Wako) at different time points after being immunized. The mice were perfused with 20 mL of cold PBS, after which their livers and spleens were harvested. The livers were sliced using scissors and crushed in a Petri dish with a syringe plunger. Liver cell suspensions were passed through a 196-μm stainless mesh. After centrifugation at 430 × g for 5 min at room temperature, the pellets were suspended in a solution of 35%

isotonic Percoll (GE Healthcare, Chicago, IL, USA). The cells were then centrifuged at $500 \times g$ for 30 min at room temperature with no brake. Parenchymal cells and debris were removed using a disposable pipette, and the pellet was suspended in Gey's solution to lyse the red blood cells. Liver cell suspensions were then passed through a 70- μm mesh. The spleens were crushed in a Petri dish using a syringe plunger. Spleen cell suspensions were then passed through a 70- μm mesh and treated with Gey's solution to lyse the red blood cells.

2.8 Flow cytometry analysis

The cells were stained with Zombie-Aqua (BioLegend, San Diego, CA, USA) for 15 min at room temperature in the dark to identify and exclude dead cells from the analysis. After being washed, the cells were stained with T-Select H-2K^b OVA Tetramer-SIINFEKL-PE (MBL, Tokyo, Japan) or T-Select H-2K^d malaria Pb9 Tetramer-SYIPSAEKI-PE (MBL) for 30 min at 4°C in the dark. The cells were then washed and stained for 30 min at 4°C in the dark to identify cell surface molecules with monoclonal antibodies. The antibodies included APC-anti-CD3e (145-2C11), BV785-anti-CD3e, FITC-anti-CD8 (KT15), APC-R700-anti-CD44 (IM7), BV421-anti-CD62L (MEL-14), BV785-anti-CD127 (A7R34), APC-anti-CD69 (H1.2F3), and BV650-anti-KLRG1 (2F1). All of the antibodies were purchased from BioLegend, BD Biosciences, or MBL. The stained cells were fixed with 1% paraformaldehyde (Wako) and analyzed using the BD FACSCelesta Flow Cytometer (BD Biosciences) and FlowJo software (BD Biosciences).

Intracellular staining was performed according to the manufacturer's instructions (BD Biosciences). The cells ($1.5\text{--}3 \times 10^6/\text{mL}$) were stimulated for 6 h with 1 mg/mL of the SIINFEKL peptide in RPMI-1640 medium with L-Glutamine and Phenol Red (Wako) supplemented with 10% heat-inactivated fetal bovine serum (FBS), penicillin/streptomycin, non-essential amino acids (0.1 mM), sodium pyruvate (1 mM), and 2-mercaptoethanol (5×10^{-5} M) with GolgiPlug (BD Biosciences) for the last 4 h. The cells were then stained with Zombie-Aqua for 15 min at room temperature in the dark to identify and exclude dead cells from the analysis. After adding the Fc receptor blocker (2.4G2), the cells were stained with the BV785-anti-CD3e, FITC-anti-CD8, and BV421-anti-CD107a monoclonal antibodies or BV421-Rat IgG2b Isotype Control. The cells were fixed, permeabilized with the BD Cytotfix/Cytoperm Fixation/Permeabilization kit (BD Biosciences), and stained with APC-anti-IFN- γ (XMG1.2), BV650-anti-TNF- α (MP6-XT22), APC, PE-anti-Granzyme B (QA16A02), or their isotype controls. The cells were then analyzed using FACSCelesta and the FlowJo software.

2.9 Serum ALT levels and anti-OVA IgG titers

The serum alanine aminotransferase (ALT) levels of the immunized mice were measured using an automatic analyzer

(Fuji DRI-chem 3500V; FUJIFILM, Tokyo, Japan). The levels of anti-OVA IgG antibodies in the sera were determined using an enzyme-linked immunosorbent assay (ELISA), as previously described (34). In brief, ELISA plates were coated with 100 $\mu\text{g}/\text{well}$ of the OVA protein (Wako) in PBS overnight at 4°C. The coated plates were washed with PBS containing 0.05% Tween 20 (washing buffer) and blocked with PBS containing 10% FBS for 30 min at room temperature. After the wash, serum ($\times 40$) was added to the plates, which were then incubated overnight at 4°C. The plates were washed, incubated with biotin-conjugated goat anti-mouse IgG-Fc fragment antibodies (Bethyl Laboratories, Montgomery, TX, USA) for 1 h at room temperature, washed, and then incubated with horseradish peroxidase-conjugated streptavidin (BioLegend) for 30 min at room temperature. After the wash, 1 \times TMB substrate solution (Thermo Fisher Scientific) was added to each well, and the plates were incubated at room temperature for 15 min. Phosphoric acid (2 M) was used to stop the reaction, and the absorbance was read at 450 and 570 nm using an iMark Microplate Absorbance Reader (Bio-Rad, Hercules, CA, USA).

2.10 Parasites and infection

Recombinant *Plasmodium berghei* ANKA (PbA) expressing GFP (PbA-GFP) and recombinant *P. berghei* 676m1c1 line (Pb-lucGFP) were used (35–37). Sporozoites were obtained from the salivary glands of infected female *Anopheles stephensi* mosquitoes 21–23 days after blood meal feeding. The mice were intravenously infected with 200 PbA-GFP sporozoites, as previously described (38). Parasitaemia levels were determined based on the expression of GFP using a BD FACSCelesta Flow Cytometer 3 days after the infections. Another group of mice were intravenously infected with 3000 Pb-lucGFP sporozoites. Forty-four hours after infection, the mice were administered 150 mg/kg of D-luciferin intraperitoneally and anaesthetized with a mixture of oxygen and isoflurane. Ten minutes later, the mice were imaged using IVIS Lumina II with an exposure time of 3 min. Bioluminescent signals in the regions of interest were quantified using Living Image 3.0. The levels of parasitemia were determined using a microscopic examination of standard thin blood smears stained with Giemsa.

2.11 CD8 depletion

Each mouse was intraperitoneally administered 100 μg of anti-mouse CD8a antibody (2.43) or rat IgG2b isotype control (LTF-2) 1 day before the induction of the sporozoite infections. Both antibodies were purchased from Bio X Cell (Lebanon, NH, USA).

2.12 Statistical analysis

Statistical analyses were performed using the GraphPad Prism software (version 8). All data were tested for normal distribution using the Shapiro–Wilk test. For comparisons between two groups,

Welch's t-test was used to assess statistical significance if the sample data followed a normal distribution; otherwise, the Mann–Whitney U test was used. For comparisons between more than two groups, a one-way or two-way ANOVA with Bonferroni's *post-hoc* test was performed if the sample data followed a normal distribution; otherwise, the Kruskal–Wallis and Dunn's *post-hoc* tests were performed.

3 Results

3.1 Preferential expression of mRNA carried by LNPs in the liver

We generated LNPs composed of four types of lipids, including SS-cleavable pH-activated lipid-like material (ssPalm), 1,2-dioleoyl-sn-glycero-3-phosphocholine (DOPC), 1,2-dimyristoyl-rac-glycero-3-methylpolyoxyethylene (DMG-PEG2000), and cholesterol. ssPalm contains dual sensing motifs that consist of a tertiary amine and disulfide bond that can respond to the intracellular environment, such as acidic conditions in the endosome and reductive conditions in the cytosol (39). We prepared LNPs with SS-OP, which is the third generation of ssPalm and has an oleic acid scaffold and a phenyl ester linker with anti-inflammatory and self-degradable properties (39). First, we used LNPs carrying firefly luciferase (FLuc) reporter mRNA (FLuc mRNA-LNPs) to determine the target tissue of the LNPs (Table 1). To determine the distribution of the LNPs, BALB/c mice were used as the pigment from darker-haired small animals can reduce bioluminescent signals. Three groups of mice were injected with FLuc mRNA-LNPs intravenously, intramuscularly, or subcutaneously, and the bioluminescence intensity of the total body and upper abdominal regions were examined 1–96 h after the injections (Figure 1A). The mice that received an intravenous injection exhibited the strongest FLuc expression in the liver, with a peak response 3 h after the injection. The mice that received intramuscular and subcutaneous injections exhibited lower FLuc expression than those receiving intravenous injections, with a delayed peak 6 h after the injections. FLuc expression levels were higher after the intramuscular injections than after the subcutaneous injections. Following the intramuscular and subcutaneous injections, FLuc expression was detected around the administration sites. To assess the immune responses in the mice, we used ovalbumin (OVA) as a model antigen. OVA has a dominant CD8⁺ T cell epitope that is restricted by H-2k^b. We removed each organ from the C57BL/6N (B6) mice that had been administered FLuc mRNA-LNPs intravenously and performed an *ex-vivo* imaging analysis 3 h after the injections (Figure 1B and Supplementary Figure 1). The FLuc signals in the liver showed the

highest intensity, whereas those in the spleen, intestines, and kidney were marginal.

3.2 Intravenous injections of OVA mRNA-LNPs activated OVA-specific CD8⁺ T cells and induced resident memory CD8⁺ T cells in the liver

To assess the immunogenicity of the mRNA-LNPs in the liver, we used OVA-specific T-cell receptor (TCR) transgenic mice, hereafter referred to as “OT-I” mice (31). B6 mice were administered 1×10^6 CD8⁺ T cells from CD45.1⁺ OT-I mice (OT-I cells) and intravenously immunized with OVA mRNA-LNPs (n = 3). Seven days after immunization, the proportion of OT-I cells within the CD8⁺ T cells reached $56.6 \pm 8.3\%$ in the livers of the mice immunized with 2 μg of OVA mRNA (Figure 2). Although the OT-I cells increased in both the liver and spleen in a dose-dependent manner, their increase was greater in the liver than in the spleen (Figure 2). These results indicate that OVA mRNA-LNPs activate OT-I cells and induce their proliferation. After confirming the immunization effects of the mRNA-LNPs in the liver, we examined whether the OVA mRNA-LNPs would induce endogenous OVA-specific CD8⁺ T cells in B6 mice. Seven days after immunization, tetramer-positive OVA-specific CD8⁺ T cells and their CD44^{hi} CD62L^{lo} CD127⁺ effector phenotypes increased in both the liver and spleen in a dose-dependent manner. The numbers of tetramer-positive cells and their effector phenotypes in the liver were greater than those in the spleen (Figures 3A, B and Supplementary Figures 2A, 3A, B). Serum alanine aminotransferase (ALT) levels were further measured to evaluate the extent of liver injury in the immunized mice. Although the ALT levels in the mice immunized with 10 μg of OVA mRNA were higher than those in the control mice, no significant differences were observed between the mice immunized with 5 μg of OVA mRNA or less and the control mice (Figure 3C). We therefore used 5 μg of OVA mRNA-LNPs for the subsequent experiments.

To assess whether the OVA mRNA-LNPs could induce OVA-specific T_{RM} cells, B6 mice were immunized once with OVA mRNA-LNPs intravenously. One month after immunization, OVA tetramer⁺ CD8⁺ T cells remained in the liver and spleen, with their proportion in the liver being higher than that in the spleen (Figure 3D). T_{RM} cells (CD8⁺ CD44^{hi} CD62L^{lo} CD69⁺ KLRG1⁺) comprised $48.4 \pm 13.1\%$ of the OVA tetramer⁺ CD8⁺ T cells in the liver, but there were few T_{RM} cells in the spleen (Figure 3E and Supplementary Figures 2B, 3C, D). Effector memory CD8⁺ T cells (T_{EM}) (CD8⁺ CD44^{hi} CD62L^{lo} CD69⁺) comprised $37.9 \pm 14.9\%$ and central memory CD8⁺ T cells (T_{CM}) (CD8⁺ CD44^{hi} CD62L^{hi}) comprised $6.8 \pm 3.5\%$ of the tetramer⁺

TABLE 1 Physicochemical properties of LNPs.

Size (z-average) (nm)	PDI*	Zeta potential (mV)	EE** (%)
94.8 ± 2.7	0.070 ± 0.012	-2.13 ± 0.84	97.1 ± 1.61

*PDI, polydispersity index; **EE, Encapsulation efficiency. Data represent mean ± S.D. (n = 3).

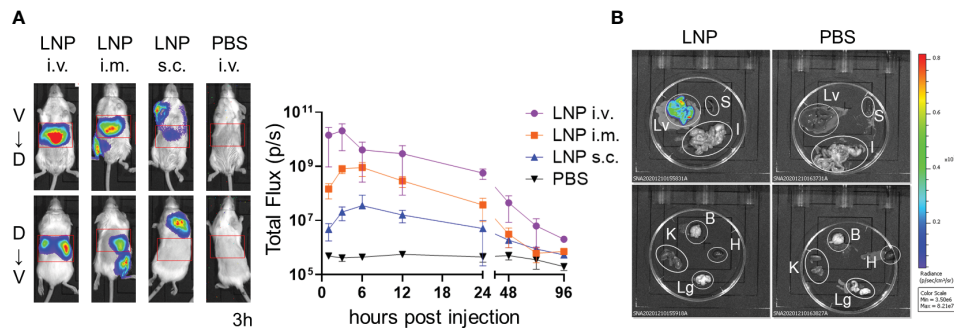


FIGURE 1 Distribution of LNPs in the mice. **(A)** Temporal expression of FLuc mRNA. BALB/c mice were injected with LNPs containing 5 μ g of FLuc mRNA (5 μ g of FLuc mRNA-LNPs) intravenously, intramuscularly, or subcutaneously (n = 3). As a negative control, another group of mice were intravenously injected with 100 μ L of PBS. Bioluminescence was measured 1, 3, 6, 12, 24, 48, 72, and 96 h post injection. Representative images of ventrodorsal (V→D) and dorsabdrominal (D→V) shootings taken 3 h after the injection are shown on the left. A summary graph of the total flux [photons/s] in the liver is shown on the right. Data represent the mean \pm SD. **(B)** FLuc expression in organs. B6 mice were intravenously injected with LNPs containing 5 μ g of FLuc mRNA or 200 μ L of PBS (n = 4). The liver, spleen, gastrointestinal tract, kidneys, brain, heart, and lungs were collected 3 h after injection, and bioluminescence was measured. Representative images for each organ are shown. Lv, Liver; S, Spleen; I, gastrointestinal tract; B, Brain; K, Kidney; H, Heart; Lg, Lung.

CD8⁺ T cells in the liver (Supplementary Figures 3C, D). In the spleen, OVA-specific CD8⁺ T cells consisted of 3.7 \pm 1.4% T_{RM} cells, 50 \pm 7.3% T_{EM} cells, and 33.3 \pm 10.5% T_{CM} cells. The number of liver T_{RM} cells was maintained for more than 2 months after immunization (Figures 3D, E). To investigate the effector function of the memory CD8⁺ T cells in the liver, we performed intracellular cytokine staining 1 month after immunization (Supplementary Figure 4). An *in-vitro* stimulation with the SIINFEKL peptide, which is an MHC class I dominant epitope of OVA, detected IFN- γ ⁺ and INF- γ ⁺ TNF- α ⁺ double-producing CD8⁺ T cells in the livers of the immunized mice (Supplementary Figure 4A). In addition, the co-expression of Granzyme B and the degranulation

marker CD107a was induced in the CD8⁺ T cells in response to the SIINFEKL peptide stimulation (Supplementary Figure 4B). Collectively, these data suggest that a single dose of OVA mRNA-LNPs can induce OVA-specific T_{RM} cells, which may possess multifunctional effector activity.

Next, we examined whether immunization via intramuscular and subcutaneous routes would induce OVA-specific T_{RM} cells in the liver. Seven days after immunization, the levels of OVA-specific CD8⁺ T cells in the livers of the mice immunized via intramuscular and subcutaneous routes were not significantly different from those immunized intravenously, whereas the levels of OVA-specific CD8⁺ T cells in the spleen were higher in the mice immunized

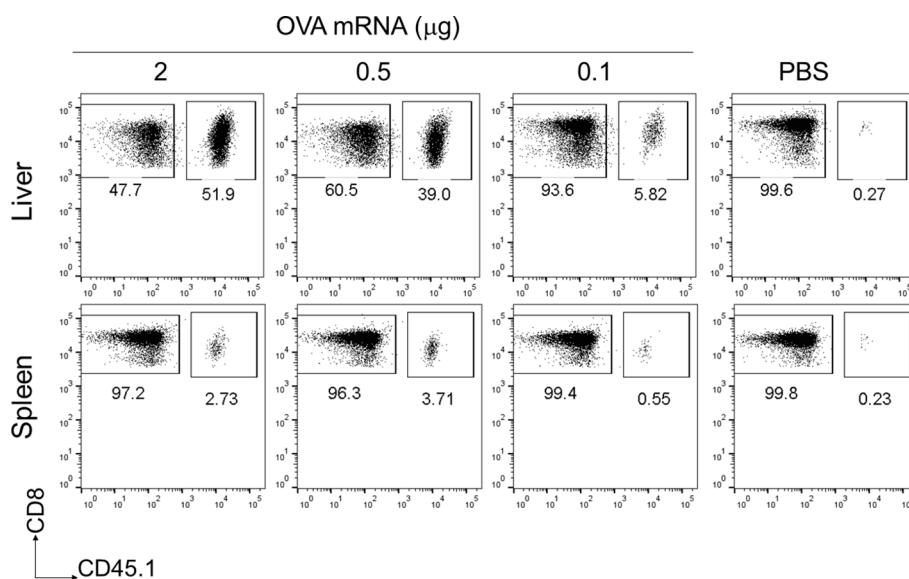


FIGURE 2 OT-I cells were strongly activated in the liver following a single intravenous injection of OVA mRNA-LNPs. CD45.1⁺ OT-I cells (1 \times 10⁶) were adoptively transferred to B6 mice. Two days after cell transfer, the mice were intravenously injected with serial doses of OVA mRNA-LNPs or PBS (n = 3). Seven days post injection, the mice were analyzed. Representative dot plots show the proportion of OT-I in CD3⁺CD8⁺ cells within the liver (upper panel) and spleen (lower panel).

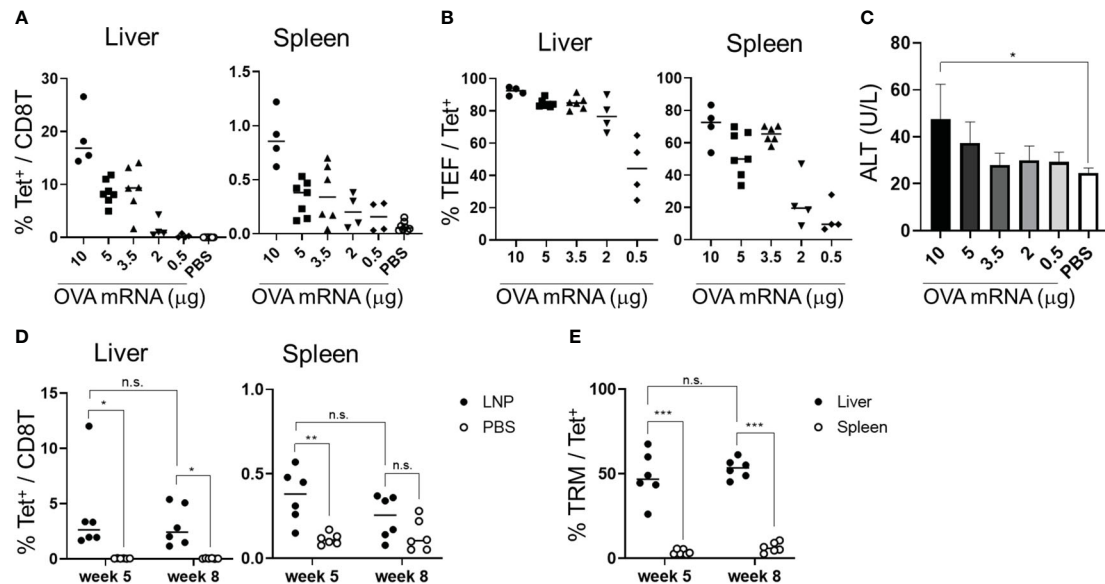


FIGURE 3

OVA mRNA-LNPs induced OVA-specific CD8⁺ T cells and memory cells in the liver. (A–C) B6 mice were intravenously injected with the indicated doses of OVA mRNA-LNPs or 200 µL of PBS. Seven days after injection, the mice were analyzed. The proportion of H-2K^b SIINFEKL-restricted tetramer⁺ within the CD8⁺ T cells in the liver (left) and spleen (right) is shown (A). The proportion of effector (CD127[−] CD44^{hi} CD62L^{lo}) cells within the tetramer⁺ cells in the liver (left) and spleen (right) is shown (B). The serum ALT levels on day 7 are shown in (C). (D, E) B6 mice were intravenously injected with 5 µg of OVA mRNA-LNPs or 200 µL of PBS (n = 6). One and two months after injection, the mice were analyzed. The proportion of tetramer⁺ CD8⁺ T cells in the liver (left) and spleen (right) is shown (D). The proportion of T_{RM} (CD44^{hi} CD62L^{lo} CD69⁺ KLRG1[−]) cells within the tetramer⁺ cells in the liver (left) and spleen (right) is shown (E). These results were obtained from three (A–C) and two experiments (D, E). The data represent the mean (A, B, D, E) or the mean ± SD (C); *P < 0.05, ***P < 0.001, n.s. (not significant), as indicated by a one-way ANOVA with Bonferroni's post-hoc test (C) and Mann–Whitney U test (D, E).

subcutaneously than in those immunized intravenously (Figure 4A). The proportions of OVA-specific CD8⁺ T cells with the effector phenotype (CD44^{hi} CD62L^{lo} CD127[−]) that were induced in the liver following intravenous, intramuscular, and subcutaneous immunization were at similar levels (90.4 ± 4.2, 88.38 ± 1.8, and 87.1 ± 2.5%, respectively; Figure 4B, Supplementary Figures 2A, 5). After 1 month, the levels of OVA-specific T_{RM} cells were evaluated in the mice immunized via different routes. The proportions of OVA-specific CD8⁺ T cells in the livers of the intravenously-immunized mice were comparable to those in the intramuscularly-immunized mice and higher than those in the subcutaneously-immunized mice (Figure 4C). The proportion of T_{RM} cells in the liver was highest in the mice immunized intravenously, followed by those immunized intramuscularly (Figure 4D and Supplementary Figure 6). In contrast, the majority of the tetramer⁺ cells in the liver were T_{EM} cells when the mice were immunized subcutaneously (Supplementary Figure 6B). In the spleen, OVA-specific memory CD8⁺ T cells were poorly induced by all three forms of immunization and were mainly T_{EM} and T_{CM} cells (Figures 4C, D; Supplementary Figure 6). Additionally, we tested the levels of IgG specific to the OVA protein to confirm the induction of humoral immunity by the mRNA-LNPs. Compared with the phosphate-buffered saline (PBS) control, the subcutaneous injections induced significantly higher levels of anti-OVA IgG antibodies, whereas the intravenous and intramuscular injections did not (Supplementary Figure 7). Taken together, these results

indicate that the intravenous route was the most effective in inducing specific T_{RM} cells in the liver, followed by the intramuscular and subcutaneous routes; however, when considering the practical applications of human vaccines, the intramuscular route may be more feasible.

3.3 Intramuscular immunization in BALB/c mice with CSP mRNA-LNPs protected against *Plasmodium berghei* ANKA sporozoites

To determine the efficacy of vaccinations with *Plasmodium* antigens and CSPs, we immunized BALB/c mice with PbA CSP mRNA as the dominant MHC class I epitope of PbA CSP is present on H-2K^d and not on K^b or D^b (Figure 5A). The NANP repeat region of the CSP was excluded from the construct as we mainly aimed to induce a cell-mediated protective immune response. The BALB/c mice were immunized intramuscularly with CSP mRNA-LNPs twice at 3-week intervals. As a negative control, another group of mice were immunized with OVA mRNA-LNPs. The proportion of CSP-specific CD8⁺ T cells significantly increased in the livers of the CSP mRNA-LNP-immunized mice 33 days after the last immunization; 35.5 ± 7.2% of the cells were T_{RM} cells (Figures 5B, C and Supplementary Figure 8). One month after the second immunization, the mice were administered with 200 GFP-expressing PbA (PbA-GFP) sporozoites. Half of the immunized

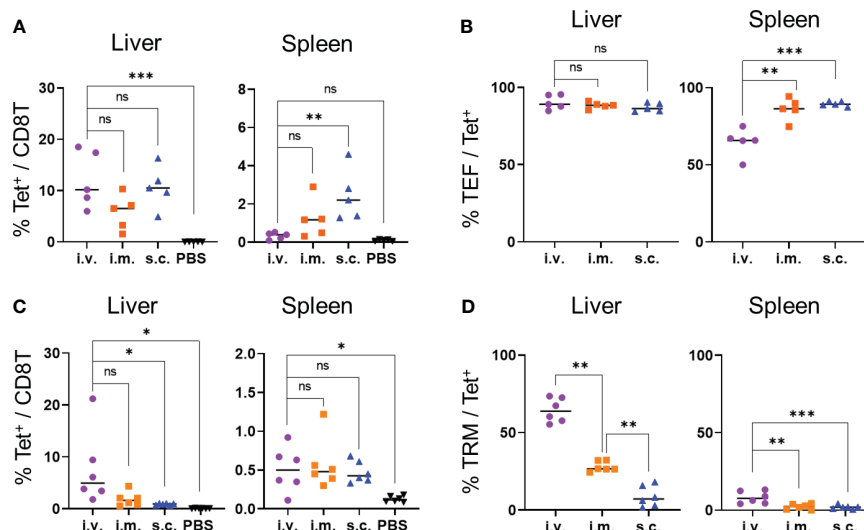


FIGURE 4

T_{RM} cell generation was affected based on the injection routes of the OVA mRNA-LNPs. B6 mice were injected with 5 μ g of OVA mRNA-LNPs intravenously (i.v.), intramuscularly (i.m.), or subcutaneously (s.c.). As a negative control, another group of mice were intravenously injected with 100 μ L of PBS. (A, B) Seven days after injection, the mice were analyzed ($n = 5$). The proportion of tetramer⁺ CD8⁺ T cells in the liver (left) and spleen (right) is shown in (A). The effector (CD127⁻ CD44^{hi} CD62L^{lo}) cells within the tetramer⁺ cells in the liver (left) and spleen (right) are shown (B). (C, D) One month after injection, the mice were analyzed ($n = 6$). The proportion of tetramer⁺ CD8⁺ T cells in the liver (left) and spleen (right) is shown (C). T_{RM} (CD44^{hi} CD62L^{lo} CD69⁺ KLRG1⁻) cells within the tetramer⁺ cells in the liver (left) and spleen (right) are shown (D). These results were obtained in two experiments. Data represent the mean; * $P < 0.05$, ** $P < 0.01$, *** $P < 0.001$, n.s. (not significant), as indicated by a one-way ANOVA with Bonferroni's *posthoc* test.

mice (three out of six) exhibited sterile immunity, and the onset of the blood stage was delayed by 2 days in the other mice when compared with the negative control mice (Figure 5D). To confirm that immunization with CSP mRNA-LNPs provides protection during the liver-stage malaria, the parasite burden in the liver was determined using luciferase- and GFP-expressing *P. berghei* (Pb-lucGFP). BALB/c mice were immunized twice with N1-methylpseudouridine CSP (Ψ -CSP) mRNA-LNPs at 3-week intervals and challenged with 3000 Pb-lucGFP sporozoites 5 weeks after the final immunization. Forty-four hours after infection, luciferase activity was monitored using IVIS. The expression levels of luciferase in Ψ -CSP-immunized mice were significantly lower than those in the control mice (Figure 5E). We also evaluated the longevity of the efficacy of CSP mRNA-LNPs 9 and 13 weeks after the final immunization (Supplementary Figure 9). Protective immunity against the sporozoite infection in the mice immunized with Ψ -CSP persisted for at least 13 weeks after final the immunization.

To confirmed that this protection is dependent on CD8⁺ T cells, Ψ -CSP mRNA-LNP immunized mice were administrated anti-mouse CD8 antibodies 1 day before the sporozoite infection to deplete CD8⁺ T cells. As a negative control, Ψ -CSP mRNA-LNP immunized mice were administrated control IgG 1 day before the sporozoite infection. These mice were infected with 3000 Pb-lucGFP sporozoites. Forty-four hours after infection, the control IgG-treated mice exhibited significantly lower levels of luciferase expression than the unimmunized mice (Figure 6). In contrast, the anti-CD8-treated mice exhibited luciferase expression levels that were similar to those in the unimmunized mice and higher than those in the control IgG-treated mice, although the latter results were not significant. These results indicate that CD8⁺ T cells played

a crucial role in the protection against sporozoite infection in mice immunized with CSP mRNA-LNPs. Taken together, these results suggest that mRNA-LNPs have the potential to be used in malaria vaccines for clinical use.

4 Discussion

RAS is a well-established malaria vaccine model that provides sterile protection in rodent models and humans infected with *P. falciparum* (11, 15). The major mechanisms of action of RAS include the induction of cytotoxic T cells residing in the liver, which terminate the liver-stage propagation of *P. falciparum* and antibodies that block the invasion of sporozoites into hepatocytes (19). In this study, we aimed to develop a malaria vaccine that efficiently induces cellular immunity in the liver. We found that mRNA-LNPs targeted the expression of its coding protein in the liver and induced antigen-specific liver T_{RM} cells through intravenous or intramuscular injections. Generally, LNPs are thought to accumulate in the liver when administered systemically via intravenous and intramuscular injections (27, 29, 30). This is likely because the liver is a site for lipid metabolism. It has been shown that liver T_{RM} cells can be induced by targeting antigens to the liver using the “prime and trap vaccination” method, in which antigen-specific CD8⁺ T cells are activated in primary lymphoid organs at the “prime” step and targeted to the liver using antigen peptide-expressing recombinant adeno-associated viruses in the “trap” step (22, 40, 41). mRNA-LNPs target antigens in the liver and are therefore an ideal method of choice to induce T_{RM} cells in the liver.

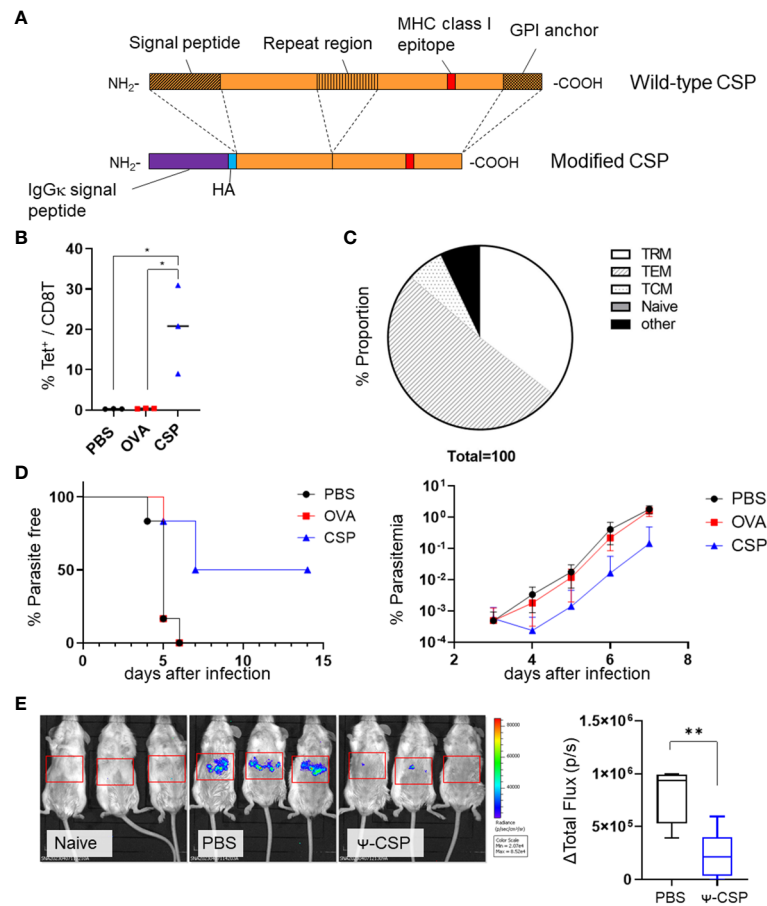


FIGURE 5

Sterile immunity against the PbA sporozoite was induced by PbA circumsporozoite protein (CSP) mRNA-LNPs. **(A)** Structure of the modified CSP. The signal peptide, repeat region (B-cell epitope), and GPI anchor were deleted from the wild-type CSP, and signal peptides of IgGκ and HA tags were inserted to create modified CSP. **(B)** BALB/c mice were injected with 3.35 μg of CSP, 5 μg of OVA mRNA-LNPs, or 100 μL of PBS intramuscularly twice at 3-week intervals. One month after the final injection, the proportion of tetramer⁺ cells within the CD8⁺ T cells in the liver was observed. **(C)** The proportions of T_{RM} (CD44^{hi} CD62L^{lo} CD69⁺ KLRG1⁻), T_{EM} (CD44^{hi} CD62L^{lo} CD69⁻), T_{CM} (CD44^{hi} CD62L^{hi}), naïve (CD44^{lo} CD62L^{hi}), and other cell populations within the tetramer⁺ cells in the livers of the mice immunized with CSP mRNA-LNPs are shown. **(D)** Mice immunized with CSP mRNA-LNPs were infected with 200 PbA-GFP sporozoites. The left graph shows the proportion of uninfected mice (less than 0.005% of parasitaemia). Parasitaemia 3–7 days after infection is shown on the right side. **(E)** BALB/c mice were intramuscularly injected with 6.7 μg of N1-methyl-pseudouridine CSP (ψ-CSP) mRNA-LNPs or 100 μL of PBS twice at 3-week intervals (n = 6). One month after final injection, the mice were infected with 3000 Pb-lucGFP sporozoites. Forty-four hours after infection, bioluminescence was measured. Representative images of ventrodorsal shootings are shown on the left. A summary graph of the total flux [photons/s] in the liver is shown on the right. The results were obtained across two experiments. **(B)** The data represent the mean; *P < 0.05, **P < 0.01, Kruskal–Wallis test with Dunn's *post-hoc* test. **(D)** The data represent the mean of parasitaemia ± SD. The Kruskal–Wallis test with Dunn's *post-hoc* test was performed 3–7 days after infection. Compared to the PBS group, the PbCSP group exhibited significantly lower parasitaemia 4–7 days after infection (P < 0.01). Compared with the OVA group, the PbCSP group exhibited significantly lower parasitaemia 6 and 7 days after infection (P < 0.05). **(E)** The data represent the mean ± SD; **P < 0.01, as indicated by a Mann–Whitney U test.

It has been reported that *P. falciparum* CSP (PfCSP) mRNA-LNP vaccinations substantially protect against infections caused by transgenic *P. berghei* sporozoites expressing PfCSP (42). The mRNA construct in these vaccines includes a NANP B-cell epitope that is intended to provoke an effective antibody, particularly an anti-NANP antibody. In the study that developed the vaccines, the researchers analyzed cytokine production from splenocytes stimulated with PfCSP ex-vivo. In our study, we confirmed that protective immunity can be induced by PbA CSP mRNA without the NANP sequence that includes B-cell epitope and that the protection against sporozoite infection depends on CD8⁺ T cell by treatment with anti-CD8 antibody.

Moreover, we observed marked CSP-specific T_{RM} generation in the liver. We focused on the cellular immunity in the liver, especially liver T_{RM}.

In our LNPs, SS-OP was utilized as an ionizable lipid that plays an important role in delivering LNPs into the cytoplasm of a target cell. SS-OP is the third generation of ssPalm, which has two types of units composed of a tertiary amine and disulfide bond to accelerate the degradation of LNPs, thereby resulting in the efficient delivery of nucleic acids into the cytosol (39). SS-OP has an oleic acid scaffold and a phenyl ester linker and has exhibited anti-inflammatory and self-degradable properties that allow for the efficient release of mRNA (43, 44). Compared with DLin-MC3-

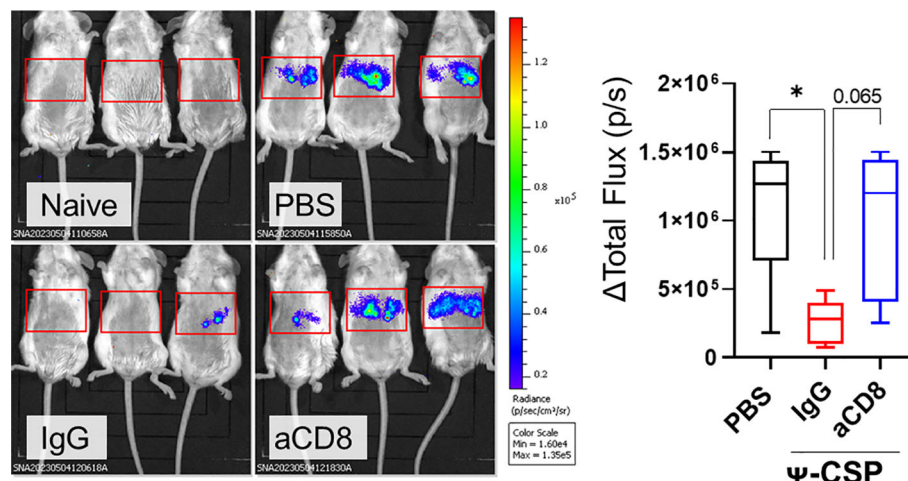


FIGURE 6

CD8⁺ T cells played a pivotal role of the protection against sporozoite infection in the mice immunize with CSP mRNA-LNPs. BALB/c mice were intramuscularly injected with 6.7 μ g of Ψ -PbCSP mRNA-LNPs or 100 μ L of PBS twice at 3-week intervals. One month after the final injection, the mice immunized with Ψ -CSP mRNA-LNPs were intraperitoneally administrated 100 μ g of anti-CD8 antibodies to deplete CD8⁺ T cells ($n = 5$). The other mice immunized with Ψ -CSP mRNA-LNPs were intraperitoneally administrated 100 μ g of control rat IgG2b as a control ($n = 5$). One days after the antibody treatment, the mice were infected with 3000 Pb-lucGFP sporozoites. Forty-four hours after infection, bioluminescence was measured. Representative images of ventrodorsal shootings are shown on the left. A summary graph of the total flux [photons/s] in the liver is shown on the right. The results were obtained across three experiments. The data represent the mean \pm SD; * $P < 0.05$, as indicated by a one-way ANOVA with Bonferroni's *post-hoc* test.

DMA, which is an ionizable lipid that was used in the first-approved siRNA-based drug (ONPATRO[®]) and has a tertiary amine, SS-OP efficiently delivered mRNA into the liver (43). Our LNPs that were composed of SS-OP likely induced a large amount of antigen expression in the liver without excessive inflammatory responses, which would have caused autoimmunity. Nevertheless, further assessment of our LNPs should be pursued.

The mRNA-LNPs induced stronger immune responses in the liver than in the spleen. This was likely related to the expression levels of the antigens, as shown by their predominant expression in the liver after the intravenous injections of the mRNA-LNPs. This relationship also reflected the route of immunization. One month after immunization, when antigens in the liver were highly expressed, the antigen-specific T_{RM} cells remained in the liver in higher numbers when the mice were immunized via the three different routes. Furthermore, because the intramuscular and subcutaneous injections led to the expression of antigens at the injection sites, these routes likely primed the immune response through other mechanisms, such as different kinds of antigen-presenting cells. The memory phenotype of antigen-specific CD8⁺ T cells and levels of specific antibodies also varied depending on the route of immunization. Further studies on the actual mechanisms that induced these differences are required to better understand these findings.

RAS, genetically-attenuated sporozoites (GAS), and chemically-attenuated sporozoites (CAS) in mice and humans have been reported to provide almost 100% sterile immunity at the pre-erythrocytic stage (15, 45–49). The present forms of mRNA-LNP-coding CSPs do not yield complete sterile immunity. Out of the six mice that were vaccinated with CSP mRNA, three exhibited sterile immunity, and the other three showed development of a blood stage

that was delayed by 2 days. This delayed onset of the blood stage was considered to lead to approximately 80% protection against the liver stage of malaria (50). When considering why our LNPs did not yield complete sterile protection, we determined that the number of CSP-specific T_{RM} cells was insufficient, although the possibility of a low function in the T_{RM} cells induced by the mRNA-LNPs has also been taken into account. Previous studies have shown that RASV-immunized B6 mice have approximately 10⁴ of specific T_{RM} cells in the liver and further exhibit 30% sterile immunity (22, 40, 51). This number of T_{RM} cells in the liver was similar to that of our CSP-specific T_{RM} cells in the liver. These studies have further shown that complete protection against PbA sporozoites requires 10⁵ specific T_{RM} cells in the liver. In BALB/c mice, *P. yoelii* RASV, which is a vaccine against another strain of rodent malaria, has been found to induce 70% sterile protection, although only 10² of CSP-specific T_{RM} cells in the liver have been found to be induced following the use of this vaccine (52). However, the required number of T_{RM} cells in the liver is likely to differ depending on the malarial strains causing infection. There may also be other protective factors, such as natural immunity by adjuvant effects. In such cases, even if the same levels of adaptive immunity occur, variation may further occur individually as found in a human study investigating gamma delta T cells, natural killer cells, and CD4⁺ T cells in Controlled Human Malaria Infection (53).

In conclusion, we successfully used the mRNA-LNP platform to induce antigen-specific T_{RM} cells in the liver and further induced strong protective immunity against sporozoite infections. This platform may therefore be useful in the development of new vaccine candidates to induce liver T_{RM} cells efficiently. It may further contribute to accelerating the development of T cell-based malaria vaccines.

Data availability statement

The raw data supporting the conclusions of this article will be made available by the authors, without undue reservation.

Ethics statement

The animal study was reviewed and approved by Animal Care and Use Committee of Nagasaki University.

Author contributions

SN and ShM designed the study. SN, SaM, KO, MKam, MT, AO, MKaw, AT, J-YJ, TAr, and YK conducted the experiments. SN wrote the original manuscript draft. SN, SaM, KO, AT, J-YJ, KY, KH, and ShM wrote the manuscript. All authors have reviewed and approved the final version of the manuscript. This study was supervised by HM, TAn, KY, KH, SK, and ShM. All authors contributed to the article and approved the submitted version.

Funding

SN received financial support from Center for Diversity and Inclusion, Nagasaki university for English editing, their discussions on setting up our experimental systems with lipid nanoparticles; and Mr. Tomonari Masuda and Mr. Makoto Matsumoto for their preparation of lipid nanoparticles. This study was conducted (in part) at the Joint Usage/Research Center on Tropical Disease, Institute of Tropical Medicine, Nagasaki University, Japan.

Acknowledgments

The authors would like to thank Ms. Akiko Noguchi and Ms. Ayumi Sakai for their dedication to experimental animal care; Dr. Kazumi Kimura, Ms. Ayako Arai, Ms. Sayuri Hasegawa, Dr. Shinya

Miyazaki, and Dr. Yukiko Miyazaki for providing valuable information to improve our experimental systems with mosquitoes; Dr. Koyo Nishimura and Dr. Shintaro Fumoto for their discussions on setting up our experimental systems with lipid nanoparticles; and Mr. Tomonari Masuda and Mr. Makoto Matsumoto for their preparation of lipid nanoparticles. This study was conducted (in part) at the Joint Usage/Research Center on Tropical Disease, Institute of Tropical Medicine, Nagasaki University, Japan.

Conflict of interest

SaM is an employee of SHIONOGI & CO., LTD.

This work was supported by SHIONOGI & CO., LTD. Osaka, Japan. Nagasaki University and SHIONOGI & CO., LTD. launched the Shionogi Global Infectious Division SHINE at the Institute of Tropical Medicine NEKKEN, Nagasaki University. Based on the contract for this collaboration, SHIONOGI & CO., LTD. provided funding and contributed to improving the work through frequent discussions with the authors. However, SHIONOGI & CO., LTD. had no role in the experiments, data analysis, writing, or reviewing the paper.

Publisher's note

All claims expressed in this article are solely those of the authors and do not necessarily represent those of their affiliated organizations, or those of the publisher, the editors and the reviewers. Any product that may be evaluated in this article, or claim that may be made by its manufacturer, is not guaranteed or endorsed by the publisher.

Supplementary material

The Supplementary Material for this article can be found online at: <https://www.frontiersin.org/articles/10.3389/fimmu.2023.1116299/full#supplementary-material>

References

- World Health Organization. *World malaria Report 2021*. Available at: <https://www.who.int/teams/global-malaria-programme/reports/world-malaria-report-2021>.
- Lacerda MVG, Llanos-Cuentas A, Krudsood S, Lon C, Saunders DL, Mohammed R, et al. Single-dose tafenoquine to prevent relapse of Plasmodium vivax malaria. *N Engl J Med* (2019) 380(3):215–28. doi: 10.1056/NEJMoa1710775
- Ngufor C, Govoetchan R, Fongnikin A, Vigninou E, Syme T, Akogbeto M, et al. Efficacy of broflanilide (VECTRON T500), a new meta-diamide insecticide, for indoor residual spraying against pyrethroid-resistant malaria vectors. *Sci Rep* (2021) 11(1):7976. doi: 10.1038/s41598-021-86935-3
- Rabinovich RN, Drakeley C, Djimde AA, Hall BF, Hay SI, Hemingway J, et al. malERA: An updated research agenda for malaria elimination and eradication. *PLoS Med* (2017) 14(11):e1002456. doi: 10.1371/journal.pmed.1002456
- Tse EG, Korsik M, Todd MH. The past, present and future of anti-malarial medicines. *Malaria J* (2019) 18(1):93. doi: 10.1186/s12936-019-2724-z
- van der Pluijm RW, Tripura R, Hoglund RM, Pyae Phyo A, Lek D, ul Islam A, et al. Triple artemisinin-based combination therapies versus artemisinin-based combination therapies for uncomplicated Plasmodium falciparum malaria: a multicentre, open-label, randomised clinical trial. *Lancet* (2020) 395(10233):1345–60. doi: 10.1016/s0140-6736(20)30552-3
- Talman AM, Clain J, Duval R, Menard R, Arie F. Artemisinin bioactivity and resistance in malaria parasites. *Trends Parasitol* (2019) 35(12):953–63. doi: 10.1016/j.pt.2019.09.005
- Efficacy and safety of RTS,S/AS01 malaria vaccine with or without a booster dose in infants and children in Africa: final results of a phase 3, individually randomised, controlled trial. *Lancet* (2015) 386(9988):31–45. doi: 10.1016/s0140-6736(15)00721-8
- RTS,S Clinical Trials Partnership. Efficacy and safety of the RTS,S/AS01 malaria vaccine during 18 months after vaccination: a phase 3 randomised, controlled trial in children and young infants at 11 African sites. *PLoS Med* (2014) 11(7):e1001685. doi: 10.1371/journal.pmed.1001685

10. RTS,S Clinical Trials Partnership, Agnandji ST, Lell B, Fernandes JF, Aboosolo BP, Methogo BG, et al. A phase 3 trial of RTS,S/AS01 malaria vaccine in African infants. *N Engl J Med* (2012) 367(24):2284–95. doi: 10.1056/NEJMoa1208394
11. Hoffman SL, Goh LM, Luke TC, Schneider I, Le TP, Doolan DL, et al. Protection of humans against malaria by immunization with radiation-attenuated *Plasmodium falciparum* sporozoites. *J Infect Dis* (2002) 185(8):1155–64. doi: 10.1086/339409
12. Weiss WR, Sedegah M, Beaudoin RL, Miller LH, Good MF. CD8+ T cells (cytotoxic/suppressors) are required for protection in mice immunized with malaria sporozoites. *Proc Natl Acad Sci USA* (1988) 85(2):573–6. doi: 10.1073/pnas.85.2.573
13. Sadoff JC, Ballou WR, Baron LS, Majarian WR, Brey RN, Hockmeyer WT, et al. Oral *Salmonella typhimurium* vaccine expressing circumsporozoite protein protects against malaria. *Science* (1988) 240(4850):336–8. doi: 10.1126/science.3281260
14. Schofield L, Villaquiran J, Ferreira A, Schellekens H, Nussenzweig R, Nussenzweig V. Gamma interferon, CD8+ T cells and antibodies required for immunity to malaria sporozoites. *Nat* (1987) Dec (6149) 330:664–6. doi: 10.1038/330664a0
15. Nussenzweig RS, Vanderberg J, Most H, Orton C. Protective immunity produced by the injection of x-irradiated sporozoites of *Plasmodium berghei*. *Nature* (1967) 216(5111):160–2. doi: 10.1038/216160a0
16. Weiss WR, Berzofsky JA, Houghten RA, Sedegah M, Hollindale M, Hoffman SL. A T cell clone directed at the circumsporozoite protein which protects mice against both *Plasmodium yoelii* and *Plasmodium berghei*. *J Immunol* (1992) 149(6):2103–9. doi: 10.4049/jimmunol.149.6.2103
17. Weiss WR, Mellouk S, Houghten RA, Sedegah M, Kumar S, Good MF, et al. Cytotoxic T cells recognize a peptide from the circumsporozoite protein on malaria-infected hepatocytes. *J Exp Med* (1990) 171(3):763–73. doi: 10.1084/jem.171.3.763
18. Romero P, Maryanski JL, Corradin G, Nussenzweig RS, Nussenzweig V, Zavala F. Cloned cytotoxic T cells recognize an epitope in the circumsporozoite protein and protect against malaria. *Nature* (1989) 341(6240):323–6. doi: 10.1038/341323a0
19. Cockburn IA, Seder RA. Malaria prevention: from immunological concepts to effective vaccines and protective antibodies. *Nat Immunol* (2018) 19(11):1199–211. doi: 10.1038/s41590-018-0228-6
20. Beura LK, Jameson SC, Masopust D. Is a human CD8 T-cell vaccine possible, and if so, what would it take? CD8 T-cell vaccines: to B or not to B? *Cold Spring Harb Perspect Biol* (2018) 10(9). doi: 10.1101/cshperspect.a028910
21. Yang K, Kallies A. Tissue-specific differentiation of CD8(+) resident memory T cells. *Trends Immunol* (2021) 42(10):876–90. doi: 10.1016/j.it.2021.08.002
22. Fernandez-Ruiz D, Ng WY, Holz LE, Ma JZ, Zaid A, Wong YC, et al. Liver-resident memory CD8(+) T cells form a front-line defense against malaria liver-stage infection. *Immunity* (2016) 45(4):889–902. doi: 10.1016/j.immuni.2016.08.011
23. Mackay LK, Rahimpour A, Ma JZ, Collins N, Stock AT, Hafon ML, et al. The developmental pathway for CD103(+)/CD8+ tissue-resident memory T cells of skin. *Nat Immunol* (2013) 14(12):1294–301. doi: 10.1038/ni.2744
24. Hou X, Zaks T, Langer R, Dong Y. Lipid nanoparticles for mRNA delivery. *Nat Rev Mater* (2021) 6(12):1078–94. doi: 10.1038/s41578-021-00358-0
25. Chung JY, Thone MN, Kwon YJ. COVID-19 vaccines: The status and perspectives in delivery points of view. *Adv Drug Deliv Rev* (2021) 170:1–25. doi: 10.1016/j.addr.2020.12.011
26. Guevara ML, Persano F, Persano S. Advances in lipid nanoparticles for mRNA-based cancer immunotherapy. *Front Chem* (2020) 8:589959. doi: 10.3389/fchem.2020.589959
27. Mukai H, Ogawa K, Kato N, Kawakami S. Recent advances in lipid nanoparticles for delivery of nucleic acid, mRNA, and gene editing-based therapeutics. *Drug Metab Pharmacokinet* (2022) 44:100450. doi: 10.1016/j.dmpk.2022.100450
28. Eygeris Y, Patel S, Jozic A, Sahay G. Deconvoluting lipid nanoparticle structure for messenger RNA delivery. *Nano Lett* (2020) 20(6):4543–9. doi: 10.1021/acs.nanolett.0c01386
29. Zhang NN, Li XF, Deng YQ, Zhao H, Huang YJ, Yang G, et al. A Thermostable mRNA Vaccine against COVID-19. *Cell* (2020) 182(5):1271–83.e16. doi: 10.1016/j.cell.2020.07.024
30. Pardi N, Tuyishime S, Muramatsu H, Kariko K, Mui BL, Tam YK, et al. Expression kinetics of nucleoside-modified mRNA delivered in lipid nanoparticles to mice by various routes. *J Control Release* (2015) 217:345–51. doi: 10.1016/j.jconrel.2015.08.007
31. Hogquist KA, Jameson SC, Heath WR, Howard JL, Bevan MJ, Carbone FR. T cell receptor antagonist peptides induce positive selection. *Cell* (1994) 76(1):17–27. doi: 10.1016/0092-8674(94)90169-4
32. Ogawa K, Kato N, Yoshida M, Hiu T, Matsuo T, Mizukami S, et al. Focused ultrasound/microbubbles-assisted BBB opening enhances LNP-mediated mRNA delivery to brain. *J Control Release* (2022) 348:34–41. doi: 10.1016/j.jconrel.2022.05.042
33. Miyakoda M, Kimura D, Yuda M, Chinzei Y, Shibata Y, Honma K, et al. Malaria-specific and nonspecific activation of CD8+ T cells during blood stage of *Plasmodium berghei* infection. *J Immunol* (2008) 181(2):1420–8. doi: 10.4049/jimmunol.181.2.1420
34. Nakamae S, Kimura D, Miyakoda M, Sukhbaatar O, Inoue SI, Yui K. Role of IL-10 in inhibiting protective immune responses against infection with heterologous *Plasmodium* parasites. *Parasitol Int* (2019) 70:5–15. doi: 10.1016/j.parint.2019.01.003
35. Tamura T, Kimura K, Yuda M, Yui K. Prevention of experimental cerebral malaria by Flt3 ligand during infection with *Plasmodium berghei* ANKA. *Infect Immun* (2011) 79(10):3947–56. doi: 10.1128/IAI.01337-10
36. Ploemen IH, Prudencio M, Douradinha BG, Ramesar J, Fonager J, van Gemert GJ, et al. Visualisation and quantitative analysis of the rodent malaria liver stage by real time imaging. *PLoS One* (2009) 4(11):e7881. doi: 10.1371/journal.pone.0007881. Competing Interests: The authors have declared that no competing interests exist.
37. Janse CJ, Franke-Fayard B, Mair GR, Ramesar J, Thiel C, Engelmann S, et al. High efficiency transfection of *Plasmodium berghei* facilitates novel selection procedures. *Mol Biochem Parasitol* (2006) 145(1):60–70. doi: 10.1016/j.molbiopara.2005.09.007
38. Kimura K, Kimura D, Matsushima Y, Miyakoda M, Honma K, Yuda M, et al. CD8+ T cells specific for a malaria cytoplasmic antigen form clusters around infected hepatocytes and are protective at the liver stage of infection. *Infect Immun* (2013) 81(10):3825–34. doi: 10.1128/IAI.00570-13
39. Akita H. Development of an SS-cleavable pH-activated lipid-like material (ssPalm) as a nucleic acid delivery device. *Biol Pharm Bull* (2020) 43(11):1617–25. doi: 10.1248/bpb.b20-00534
40. Valencia-Hernandez AM, Ng WY, Ghazanfari N, Ghilas S, de Menezes MN, Holz LE, et al. A Natural Peptide Antigen within the *Plasmodium* Ribosomal Protein RPL6 Confers Liver TRM Cell-Mediated Immunity against Malaria in Mice. *Cell Host Microbe* (2020) 27(6):950–962.e7. doi: 10.1016/j.chom.2020.04.010
41. Holz LE, Prier JE, Freestone D, Steiner TM, English K, Johnson DN, et al. CD8(+) T cell activation leads to constitutive formation of liver tissue-resident memory T cells that seed a large and flexible niche in the liver. *Cell Rep* (2018) 25(1):68–79.e4. doi: 10.1016/j.celrep.2018.08.094
42. Mallory KL, Taylor JA, Zou X, Waghela IN, Schneider CG, Sibilo MQ, et al. Messenger RNA expressing PfCSP induces functional, protective immune responses against malaria in mice. *NPJ Vaccines* (2021) 6(1):84. doi: 10.1038/s41541-021-00345-0
43. Tanaka H, Takahashi T, Konishi M, Takata N, Gomi M, Shlrane D, et al. Self-Degradable Lipid-Like Materials Based on “Hydrolysis accelerated by the intra-Particle Enrichment of Reactant (HyPER)” for Messenger RNA Delivery. *Adv Funct Mater* (2020) 30(34). doi: 10.1002/adfm.201910575
44. Verlengia R, Gorjao R, Kanunfre CC, Bordin S, de Lima TM, Curi R. Effect of arachidonic acid on proliferation, cytokines production and pleiotropic genes expression in Jurkat cells—a comparison with oleic acid. *Life Sci* (2003) 73(23):2939–51. doi: 10.1016/j.lfs.2003.04.003
45. Roestenberg M, McCall M, Hopman J, Wiersma J, Luty AJ, van Gemert GJ, et al. Protection against a malaria challenge by sporozoite inoculation. *N Engl J Med* (2009) 361(5):468–77. doi: 10.1056/NEJMoa0805832
46. Bijker EM, Schats R, Obiero JM, Behet MC, van Gemert GJ, van de Vegte-Bolmer M, et al. Sporozoite immunization of human volunteers under mefloquine prophylaxis is safe, immunogenic and protective: a double-blind randomized controlled clinical trial. *PLoS One* (2014) 9(11):e112910. doi: 10.1371/journal.pone.0112910
47. Beaudoin RL, Strome CP, Mitchell F, Tubergen TA. *Plasmodium berghei*: immunization of mice against the ANKA strain using the unaltered sporozoite as an antigen. *Exp Parasitol* (1977) 42(1):1–5. doi: 10.1016/0014-4894(77)90054-6
48. Kurtovic L, Reiling L, Opi DH, Beeson JG. Recent clinical trials inform the future for malaria vaccines. *Commun Med* (2021) 1(1):26. doi: 10.1038/s43856-021-00030-2
49. Mueller AK, Labaied M, Kappe SH, Matuschewski K. Genetically modified *Plasmodium* parasites as a protective experimental malaria vaccine. *Nature* (2005) 433(7022):164–7. doi: 10.1038/nature03188
50. Reeder SM, Bah MA, Tursi NJ, Brooks RC, Patel A, Esquivel R, et al. Strategic variants of CSP delivered as synDNA vaccines demonstrate heterogeneity of immunogenicity and protection from *Plasmodium* infection in a murine model. *Infect Immun* (2021) 89(10):e0072820. doi: 10.1128/IAI.00728-20
51. Holz LE, Chua YC, de Menezes MN, Anderson RJ, Draper SL, Compton BJ, et al. Glycolipid-peptide vaccination induces liver-resident memory CD8(+) T cells that protect against rodent malaria. *Sci Immunol* (2020) 5(48). doi: 10.1126/sciimmunol.aaz8035
52. Olsen TM, Stone BC, Chuenchob V, Murphy SC. Prime-and-trap malaria vaccination to generate protective CD8(+) liver-resident memory T cells. *J Immunol* (2018) 201(7):1984–93. doi: 10.4049/jimmunol.1800740
53. de Jong SE, van Unen V, Manurung MD, Stam KA, Goeman JJ, Jochems SP, et al. Systems analysis and controlled malaria infection in Europeans and Africans elucidate naturally acquired immunity. *Nat Immunol* (2021) 22(5):654–65. doi: 10.1038/s41590-021-00911-7